



Title	Protein aggregation in the frozen state induced by dropping stress
Author(s)	Torisu, Tetsuo; Maeda, Ayuko; Ito, Shuhei et al.
Citation	European Journal of Pharmaceutical Sciences. 2025, 205, p. 106996
Version Type	VoR
URL	https://hdl.handle.net/11094/100995
rights	This article is licensed under a Creative Commons Attribution 4.0 International License.
Note	

The University of Osaka Institutional Knowledge Archive : OUKA

<https://ir.library.osaka-u.ac.jp/>

The University of Osaka



Protein aggregation in the frozen state induced by dropping stress

Tetsuo Torisu^{a,*}, Ayuko Maeda^a, Shuhei Ito^a, Susumu Uchiyama^{a,b,*}

^a Department of Biotechnology, Graduate School of Engineering, Osaka University, 2-1 Yamadaoka, Suita, Osaka 565-0871, Japan

^b Exploratory Research Center on Life and Living Systems, National Institutes of Natural Sciences, 5-1 Higashiyama, Myodaiji, Okazaki, Aichi 444-8787, Japan

ARTICLE INFO

Keywords:

Protein aggregation
Mechanical stress
Interface
Freezing
Freeze-thaw
Drop

ABSTRACT

The formation of protein aggregates, which can be immunogenic and lower the efficacy and safety of protein drugs, has been an issue in biopharmaceutical development for more than a decade. Although protein drugs are often shipped as frozen material, the effect of the accidental dropping of frozen proteins, which can occur during shipping and handling, on the physical stability has not been studied. Here, a frozen Fc fusion protein was subjected to dropping stress and the increase in the aggregate concentration was evaluated. Significant increases in micron-sized aggregates were observed at $-30\text{ }^{\circ}\text{C}$ ($p \leq 0.01$), but not at $-60\text{ }^{\circ}\text{C}$. Proteins adsorbed on the vial surfaces were not remarkably detached by the action of dropping and were not the primary cause of the increase in micron-sized aggregates. When the vials were dropped, local heat generation occurred and this led to local freeze-thaw stress that induced protein aggregation. Poloxamer-188, which is known to mitigate aggregation caused by freeze-thaw stress, effectively prevented the aggregation caused by the dropping stress in the frozen state at $-30\text{ }^{\circ}\text{C}$. In addition, rapid freezing could suppress the aggregation caused by the dropping stress. The results demonstrated that dropping stress reduced the stability of proteins even in the frozen state, and they provide new insights into the formulation and freezing processes to prevent protein aggregation caused by dropping stress in the frozen state.

1. Introduction

Antibody drugs and antibody-related drugs, including Fc fusion proteins, are being actively developed (Liu, 2015; Lu et al., 2020). However, the inherent instability of therapeutic proteins, in particular the aggregation tendency, remains a challenge in the development of such proteins because the aggregates may cause immunogenicity (Pham and Meng, 2020). Therefore, the protein sequences, formulations, container closure systems, and storage conditions need to be optimized during the development of biopharmaceuticals to reduce the amount of protein aggregates and to mitigate the risk of adverse immune responses (Kizuki et al., 2023).

A wide variety of stresses to which proteins are exposed from manufacturing to administration can induce protein aggregation. Mechanical stresses, such as shaking and impacts caused by accidental dropping, can occur during manufacturing, shipping, and administration, causing protein aggregation (Wang et al., 2010). Thus, the aggregation induced by mechanical stress is recognized as a challenge in the development and use of therapeutic proteins. A previous study that investigated the mechanical stress caused by the dropping of vials of

proteins showed that when vials containing a protein solution were dropped, cavitation occurred. Cavitation bubbles were generated, which then collapsed over a short timeframe (Randolph et al., 2015). The collapse of the bubbles induced local areas with very high temperatures and formed hydroxyl radicals, resulting in protein aggregation (Randolph et al., 2015). In addition, it has been demonstrated that proteins that are adsorbed on the surface of cavitation bubbles form aggregates as the bubbles collapse (Torisu et al., 2017).

Many pharmaceutical proteins are stored in a frozen state (Singh et al., 2009) because freezing is an effective method to enhance the chemical and physical stability of the protein solutions. Because the mobility of molecules in the frozen state is considerably lower than that in the liquid state, freezing can reduce the risk of mechanical stress (Bluemel et al., 2021a). However, a freeze-concentrated matrix (FCM) exists between the ice crystals of a frozen solution in which molecules are still mobile at a temperature higher than the glass transition temperature of the FCM (T_g') (Singh et al., 2011). Many studies have demonstrated that protein instability occurs during frozen storage, especially at temperatures higher than the T_g' value, and several issues have been identified, such as the crystallization of the cryoprotectant,

* Corresponding authors at: Department of Biotechnology, Graduate School of Engineering, Osaka University, 2-1 Yamadaoka, Suita, Osaka 565-0871, Japan
E-mail addresses: tetsuo.torisu@bio.eng.osaka-u.ac.jp (T. Torisu), suchi@bio.eng.osaka-u.ac.jp (S. Uchiyama).

pressure-induced destabilization, the formation of air bubbles, and oxidation (Authelin et al., 2020). However, the effect of mechanical stresses, such as those caused by dropping, on protein stability in the frozen state has not been studied. Considering that frozen protein formulations can be exposed to mechanical stress during manufacturing, shipping, and administration, an investigation of the stability of proteins during mechanical stress in the frozen state would be useful. Moreover, recent studies have shown that mechanical stresses applied to lyophilized products led to an increase in the amount of protein aggregates after reconstitution (Fang et al., 2022; Jin et al., 2024), which also indicates the importance of studying the stability of proteins under mechanical stress in the solid state.

In the present study, the aggregation of the therapeutic protein, T-lymphocyte-associated antigen 4-Fc portion of human immunoglobulin G1 fusion protein (CTLA4-Ig), under dropping stress in the frozen state was investigated. CTLA4-Ig was frozen and dropping stress was applied at different temperatures (-30°C and -60°C) and the generated protein aggregates were evaluated. The effects of the cooling rate and the addition of a surfactant on the aggregation were also investigated. We also propose a possible mechanism for how the dropping stress induces aggregation in the frozen state.

2. Materials and methods

2.1. Materials

Butyl rubber stoppers chemically coated with silicone and 2-mL cycloolefin polymer (COP) vials were purchased from Daiwa Special Glass Co., Ltd. (Osaka, Japan). Before use, the rubber stoppers and the vials were washed three times with MilliQ water. Poloxamer 188 (Kolliphor® P 188 Bio; P188) was a gift from BASF Japan, Ltd. (Tokyo, Japan). Coomassie brilliant blue (CBB) Stain One Super was purchased from NACALAI TESQUE, Inc. (Kyoto, Japan). Unless otherwise specified, all other reagents were purchased from FUJIFILM Wako Pure Chemical Corporation (Osaka, Japan).

CTLA4-Ig (abatacept) was purchased from Ono Pharmaceutical Co., Ltd. (Osaka, Japan). To remove P188 from the formulation, CTLA4-Ig was loaded onto a Q Sepharose column (Cytiva, Marlborough, MA, USA), followed by elution with 100 mM phosphate buffer (pH 7.0) containing 400 mM NaCl. Finally, the protein solution was dialyzed against 10 mM phosphate buffer (pH 7.0). The protein concentration was then adjusted to 1.0 mg/mL by mixing with 10 mM phosphate buffer and filtered through 0.22- μm polyether sulfone (PES) filters. Phosphate buffer containing 1.6 % (w/v) P188 was also prepared and mixed with an equal volume of sample solution containing 2.0 mg/mL CTLA4-Ig to obtain samples containing 0.8 % P188. Vials were filled with 1 mL of the protein solutions, followed by capping and sealing with rubber stoppers and aluminum seal caps.

2.2. Freezing and dropping of samples

A friability tester TFT-1200 (Toyama Sangyo Co., Ltd., Osaka Japan) was modified for use at temperatures below 0°C and coupled to an incubator, TRE-100 (ESPEC Corp., Osaka, Japan) (Fig. S1). Samples were added to COP vials and frozen at a cooling rate of $-1.0^{\circ}\text{C}/\text{min}$ from 10°C to -30°C or -60°C . After the temperature of incubator reached the specified temperature, samples were incubated at the specified temperature for 1 h. Samples were also frozen at a slower cooling rate ($-0.1^{\circ}\text{C}/\text{min}$) and rapidly at a constant temperature of -30°C .

The temperature changes of the sample solutions were monitored during freezing using a MEMORY HiLOGGER LR8431 temperature logger (HIOKI, Nagano, Japan). Cooling rates were estimated from the slope of the linear regression curve of the time-temperature data before the start of ice nucleation (A in Fig. 1). The difference in temperature between A and B in Fig. 1 was employed for the estimation of the degree of supercooling.

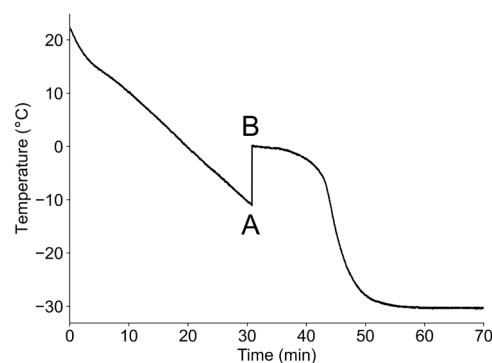


Fig. 1. Temperature change during freezing. A indicates the start of ice nucleation. B indicates the start of ice crystal growth.

After the samples were frozen, the vials were dropped and incubated at -30°C or -60°C as shown in Table S1. The vials were put into the friability tester and dropped at 50 rpm for 30, 60, and 90 min (1500, 3000, and 4500 droppings, respectively) at -30°C or -60°C . Samples dropped for 30 and 60 min were stationary incubated at -30°C or -60°C for 60 and 30 min, respectively, so that all samples were exposed to the low temperatures for 90 min. A frozen control (0 droppings) was prepared by stationary incubation at -30°C or -60°C for 90 min. Samples were thawed at 25°C for 30 min after the dropping.

2.3. Flow imaging microscopy of micron-sized aggregates

A FlowCam 8100 equipped with an 80 μm flow cell and a $10\times$ magnification lens (Yokogawa Fluid Imaging Technologies, Inc., Scarborough, ME, USA) was used to measure the concentration of aggregates $> 2 \mu\text{m}$ in equivalent spherical diameter. The sample analysis volumes were 0.15 mL and the flow rate was 0.05 mL/min. The distance to the nearest neighbor and parameter of “close holes” were set at 1 μm and 0, respectively. Particle segmentation thresholds of 15.00 were used for both dark and light pixels. Visual spreadsheet software (Yokogawa Fluid Imaging Technologies) was used for data analysis, and the particles with circularity (Hu) > 0.99 were considered as air bubbles and were not counted. The average concentrations of three vials were reported.

2.4. Size exclusion chromatography (SEC)

After thawing, 10 μL of sample solutions was injected into an Acquity ultra-performance liquid chromatography (UPLC) system (Waters, Milford, MA, USA) with a TSKgel UP-SW3000-LS column ($4.6 \times 150 \text{ mm}$; TOSOH, Tokyo, Japan). Isocratic elution was performed at room temperature at a flow rate of 0.25 mL/min with 10 mM phosphate buffer with 200 mM potassium chloride. UV absorbance at 280 nm was monitored for 12 min. The data were analyzed with Empower 3 Software (Waters, Milford, MA, USA). The relative monomer% was calculated by dividing the monomer peak area at a given time point of dropped samples with the peak area in samples not subjected to dropping. The samples were injected in triplicate and the average of three injections was calculated and reported.

2.5. Differentiation of particles from the vial surface from other particles

Experiments were conducted to investigate whether the aggregates induced by dropping came from the vial surface. First, adsorption of CTLA4-Ig on the vial surface was induced by shaking the vials filled with the protein solution for 24 h at 100 rpm using the reciprocal shaker NR-1 (TAITEC Corporation, Saitama, Japan) in the TRE-100 incubator set at 4°C . Then, the solutions were removed, and 1.5 mL of CBB dye solution filtered through 0.22 μm PES membranes was added to the vials. Then, the vials were shaken for 30 min at 100 rpm and 4°C . The dye solutions

were removed, and the vials were washed with MilliQ water seven times.

The vials that had inner surfaces coated with dyed proteins were then filled with 1 mL of non-dyed protein solution and put into the TRE-100 incubator. The samples were frozen by cooling at $-1\text{ }^{\circ}\text{C}/\text{min}$ to $-30\text{ }^{\circ}\text{C}$, incubated at $-30\text{ }^{\circ}\text{C}$ for 1 h, and dropped at $-30\text{ }^{\circ}\text{C}$ at 50 rpm for 30, 60, and 90 min (1500, 3000, and 4500 dropping cycles, respectively). The solutions were thawed and images of the generated particles were obtained using a FlowCam 8100 with a color camera. The obtained images were used as test data.

A support vector machine (SVM) was employed for the differentiation of dyed particles, which were considered to be particles from the vial surface, from non-dyed particles. Because SVM is a supervised machine learning algorithm, training and validation of a classifier were conducted. CTLA4-Ig samples with and without CBB dye were frozen and dropped at 50 rpm for 60 min. After thawing, particle images were obtained using a FlowCam 8100 with a color camera and used for the training and validation. Images of 800 particles (400 dyed particles and 400 non-dyed particles) were used for the training of the classifier. A 2D scattering plot was obtained by principal component analysis from four color- or appearance-related parameters: ratio blue/green; ratio red/blue; sigma intensity; and transparency. Then, SVM was applied to the plot to set a decision boundary. After the decision boundary was validated using another 1600 particle images (800 dyed particles and 800 non-dyed particles), the trained classifier was applied for the analysis of the test data. The number of particles classified in each class was counted.

2.6. Statistical analysis

Data are expressed as the mean or mean \pm standard deviation. One-sided Dunnett's tests were used to evaluate the increase in particle concentration after dropping compared with samples without dropping. Welch's *t*-test was used to evaluate the difference in cooling rates and degrees of supercooling between different freezing conditions. A *p*-value ≤ 0.01 was considered statistically significant.

3. Results and discussion

3.1. Protein aggregation after dropping stress at $-30\text{ }^{\circ}\text{C}$ and $-60\text{ }^{\circ}\text{C}$

CTLA-4-Ig solutions were frozen at a cooling rate of $-1.0\text{ }^{\circ}\text{C}/\text{min}$ and exposed to dropping stress at $-30\text{ }^{\circ}\text{C}$ or $-60\text{ }^{\circ}\text{C}$. As shown in Fig. 2, the amounts of aggregates $> 2\text{ }\mu\text{m}$ in diameter were significantly increased after dropping stress at $-30\text{ }^{\circ}\text{C}$ for 60 and 90 min ($p \leq 0.01$), whereas no

significant increase was observed after dropping stress at $-60\text{ }^{\circ}\text{C}$. Oligomers that could be measured by SEC were not increased by dropping stress at $-30\text{ }^{\circ}\text{C}$ (Fig. 3). The particle concentrations of the unfrozen control and samples without dropping stress were compared to evaluate the stability of CTLA4-Ig under freeze-thaw stress. A significant increase in the concentration of particles was observed after freeze-thaw stress ($p \leq 0.01$), indicating that CTLA-4-Ig was unstable under these freeze-thaw conditions. Thus, the generation of micron-sized aggregates could have occurred under freeze-thaw stress alone and was increased further by the dropping stress.

The increase in particles with sizes $> 2\text{ }\mu\text{m}$ caused by the dropping stress was prevented by the addition of P188 (Fig. 4). The particle concentration of the sample not subjected to dropping was comparable to that of the unfrozen control when P188 was added. This result indicated that P188 was effective in preventing the increase in micron-sized particles observed under the freeze-thaw stress. The protective effect of the non-ionic surfactant P188 has been shown to be a result of the surfactant inhibiting the denaturation of the protein on the ice crystals (Li et al., 2023). Considering that P188 was effective in preventing both freeze-thaw and dropping stress in the present study, the ice crystal surface is likely to be involved in the increase in the particle concentrations observed with dropping stress.

The cooling rates and supercooling can affect the size and morphology of ice crystals, and therefore the cooling rates and degrees of supercooling were monitored using a temperature logger. The cooling rates of the sample solutions were well matched with the set cooling rate of the incubator and were $-1.0\text{ }^{\circ}\text{C}/\text{min}$ for both samples cooled to $-30\text{ }^{\circ}\text{C}$ or $-60\text{ }^{\circ}\text{C}$ (Fig. 5). Before ice crystals started to form, supercooling occurred for both samples. The degrees of supercooling of samples cooled to $-30\text{ }^{\circ}\text{C}$ and $-60\text{ }^{\circ}\text{C}$ were comparable to each other: $7.1 \pm 4.6\text{ }^{\circ}\text{C}$ and $6.4 \pm 1.9\text{ }^{\circ}\text{C}$, respectively. Although the ice crystal size and morphology were not directly measured, this result suggested that there were not crucial differences in the ice crystal size and morphology between the two samples. Therefore, the difference in the increase in micron-sized aggregates between $-30\text{ }^{\circ}\text{C}$ and $-60\text{ }^{\circ}\text{C}$ could be attributed to the temperature during the dropping stress rather than to the cooling conditions.

3.2. Effect of the cooling rate on the protein aggregation caused by dropping stress in the frozen state

Protein aggregation caused by dropping stress was evaluated for samples frozen at different cooling rates to evaluate whether the ice crystal size and shape affected the aggregation. When CTLA4-Ig solutions were put into the incubator at $-30\text{ }^{\circ}\text{C}$, the cooling rate of the solutions was $-8.2 \pm 2.4\text{ }^{\circ}\text{C}/\text{min}$. The observed cooling rate of solutions frozen by cooling the incubator to $-30\text{ }^{\circ}\text{C}$ with the temperature change set at $-0.1\text{ }^{\circ}\text{C}/\text{min}$ was $-0.09 \pm 0.0\text{ }^{\circ}\text{C}/\text{min}$. The degree of supercooling of slowly frozen samples was $8.6 \pm 1.3\text{ }^{\circ}\text{C}$, which was not significantly different from that of samples cooled at $-1.0\text{ }^{\circ}\text{C}/\text{min}$, whereas the degree of supercooling of samples frozen at a constant temperature of $-30\text{ }^{\circ}\text{C}$ was relatively lower ($1.6 \pm 0.9\text{ }^{\circ}\text{C}$) than that under the other two conditions (Fig. 5).

No significant increase in the number of particles $> 2\text{ }\mu\text{m}$ was observed when the samples were frozen at either a slower ($-0.09 \pm 0.0\text{ }^{\circ}\text{C}/\text{min}$) or faster ($-8.2 \pm 2.4\text{ }^{\circ}\text{C}/\text{min}$) cooling rate, whereas the number of particles $> 2\text{ }\mu\text{m}$ was increased when samples were cooled at $-1.0\text{ }^{\circ}\text{C}/\text{min}$ (Fig. 6). This result suggested that ice crystal size and/or morphology are important factors in protein aggregation caused by dropping stress in the frozen state. For the slowly frozen sample, a significant increase was observed in the number of particles $> 5\text{ }\mu\text{m}$ ($p \leq 0.01$), while the increase in the number of particles $> 2\text{ }\mu\text{m}$ was statistically non-significant. By contrast, the number of particles $> 5\text{ }\mu\text{m}$ was not significantly increased when samples were frozen rapidly (Fig. 6). Because the size of ice crystals becomes smaller as the cooling rate is increased (Arsiccio and Pisano, 2018), the surface areas of the ice crystal

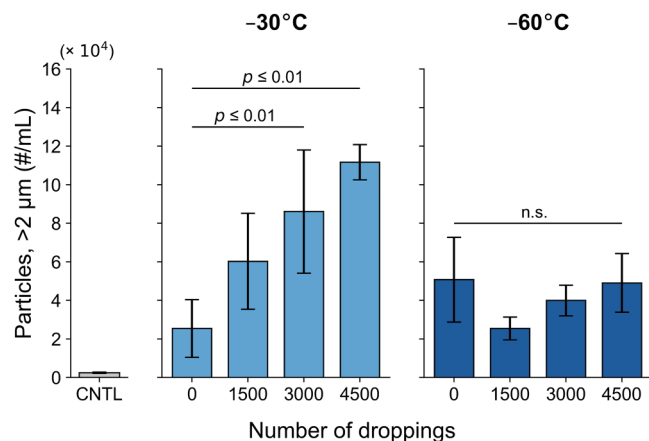


Fig. 2. Concentrations of particles $> 2\text{ }\mu\text{m}$ after applying dropping stress at $-30\text{ }^{\circ}\text{C}$ and $-60\text{ }^{\circ}\text{C}$. CNTL is the unfrozen control. n.s.: not significant. Error bars represent the standard deviation of three measurements.

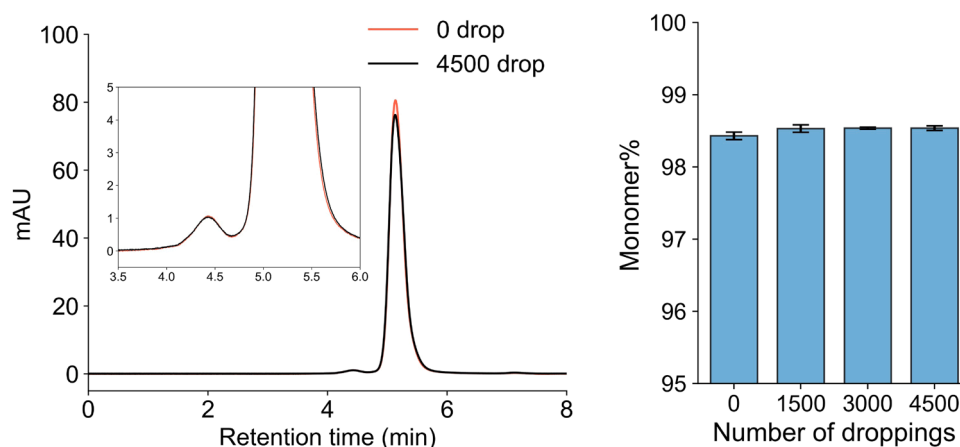


Fig. 3. Representative SEC chromatogram (left) and monomer% (right) after applying dropping stress at -30°C . The inset shows a zoomed view of part of the chromatogram. Error bars represent the standard deviation of three measurements.

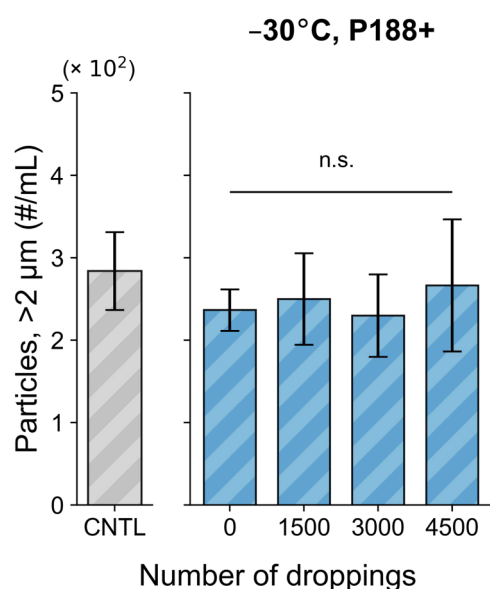


Fig. 4. Concentrations of particles $> 2\ \mu\text{m}$ after applying dropping stress to samples containing 0.8 % P188 at -30°C . CNTL is the unfrozen control. n.s.: not significant. Error bars represent the standard deviation of three measurements.

interfaces of samples frozen rapidly would be the largest of all the samples. A previous study has demonstrated that a larger surface area resulted in a larger number of aggregates (Eckhardt et al., 1991); however, in the present study, the number of micron-sized particles in samples frozen rapidly was not increased under the dropping stress. Therefore, a larger ice crystal surface area does not necessarily result in an increase in the number of protein aggregates induced by dropping stress in the frozen state. Different cooling rates can result in different ice crystal shapes. A previous report has shown that cooling rates of $0.5^{\circ}\text{C}/\text{min}$ and $1^{\circ}\text{C}/\text{min}$ generated highly branched ice dendrites, and faster cooling rates generated long needle-shaped ice with less branches (Hauptmann et al., 2019). The degree of supercooling is also an important parameter to determine ice morphology (Searles et al., 2001). Differences in ice morphology might result in the different aggregation tendencies of the samples frozen at different cooling rates.

3.3. Contribution of the vial surface to the increase in the number of aggregates in the frozen state

In addition to the ice crystal interfaces, the vial inner surface is another interface that can be involved in the formation of micron-sized aggregates (Yoneda et al., 2021). Proteins can be adsorbed on the vial inner surface before and during freezing, and these adsorbed proteins can be physically detached by the dropping stress and form aggregates. To evaluate the contribution of the vial interfaces, CTLA4-Ig was loaded onto the vial surface and dyed with CBB, then non-dyed CTLA4-Ig

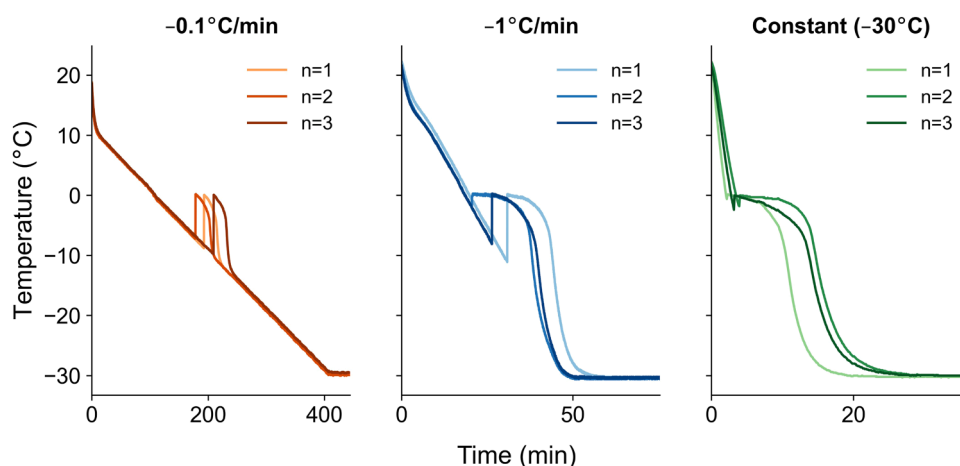


Fig. 5. Temperature changes during freezing under different freezing conditions. The measurements were repeated three times.

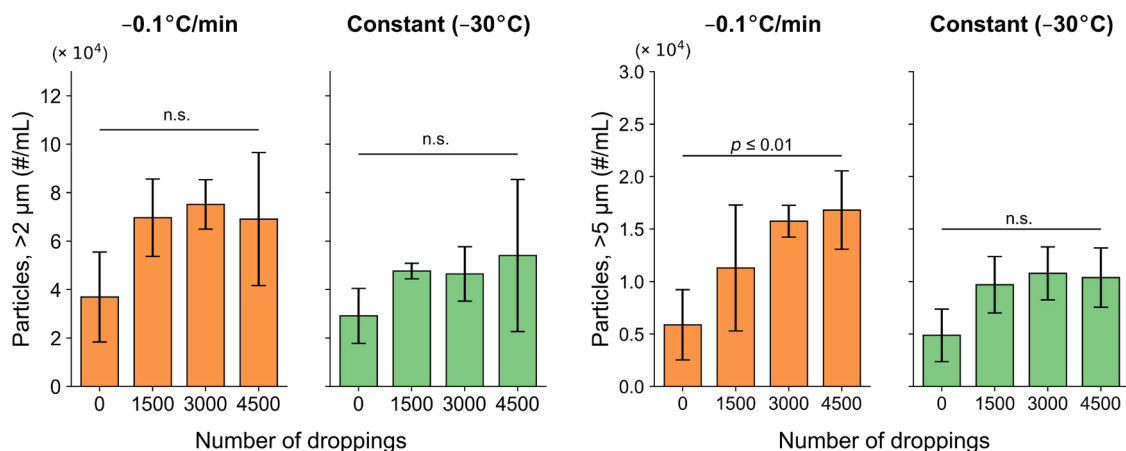


Fig. 6. Concentrations of particles > 2 μm (left) and > 5 μm (right) after applying dropping stress to samples frozen at slower (−0.1 °C/min) and faster (−30 °C, constant) cooling rates. n.s.: not significant. Error bars represent the standard deviation of three measurements.

solution was added to the vials coated with the dyed CTLA4-Ig. The vials were cooled at −1.0 °C/min to −30 °C and subjected to dropping stress that had been observed to cause an increase in micron-sized particles. After thawing, images of the aggregates were acquired using color camera equipped flow imaging microscopy.

To differentiate non-dyed particles from dyed particles derived from the vial surface, a classifier using a SVM algorithm was established. The classifier was created using particle image data obtained by applying mechanical stress to a CTLA4-Ig solution with or without CBB dye. The validation of the classifier using test data indicated that the classifier had high accuracy (95.8 %) (Fig. S2).

The established classifier was then applied to the particles obtained by applying dropping stress to samples added to vials coated with dyed CTLA4-Ig (Fig. 7). Interestingly, the number of non-dyed particles was significantly increased ($p \leq 0.01$), whereas the number of dyed particles did not show a significant increase. This result indicated that the vial surface was not the main cause of the increase in the number of micron-sized aggregates.

3.4. Possible root cause of the aggregation induced by dropping stress in the frozen state

The experiment using CBB dye indicated that the vial surface was not a major contributor to the aggregation, and therefore the aggregation was likely to occur in the frozen material. During the freezing of solutions, protein molecules experience several stresses that induce protein aggregation, including pH shifts, freeze concentration, and exposure to ice crystal interfaces (Li et al., 2021). In addition, changes in the heat capacity between the native and denatured states of a protein could result in cold denaturation. Because we used sodium phosphate buffer, a dibasic salt could crystallize during the freezing and thus the pH value of the solution could be decreased. For example, the pH value of 100 mM sodium phosphate buffer can be changed from 7 to 3 by freezing (Thorat et al., 2020). The structural stability of CTLA4-Ig can be reduced as the pH is decreased (Fast et al., 2009). A previous study has reported that the cold denaturation of monoclonal antibodies occurred at approximately −20 °C (Lazar et al., 2010). Moreover, local pressure derived from ice crystal formation can destabilize proteins (Authelin et al., 2020). Thus, there is a possibility that denaturation occurred during the freezing and this led to the aggregation. In addition, the isoelectric point of CTLA4-Ig is 4.5–5.5, and a pH shift might result in lower colloidal stability, which is a parameter closely related to aggregation (Oyama et al., 2020). The protein concentration becomes higher as ice crystals form, and aggregates can be generated under the low colloidal stability conditions. The denaturation and colloidal instability may accelerate the protein aggregation caused by dropping stress in the frozen state; however, these effects can occur at both −30 °C and −60 °C, and the reason why the aggregation was increased at −30 °C but not at −60 °C cannot be fully explained by these factors.

The ice crystal interface causes protein denaturation and aggregation (Blumel et al., 2021b). The findings that P188 prevented the aggregation effectively and that the freezing rates affected the aggregation infer that the ice crystal interface could have an important role in the aggregation under dropping stress as discussed above. Notably, a larger ice crystal surface area does not necessarily result in increased aggregates, and the ice morphology may have an impact on the aggregation. Air bubbles can also be generated during freezing. The surface of air bubbles is hydrophobic and can cause protein aggregation similar to an ice crystal interface. However, because it is difficult to accurately predict or measure the amount of air bubbles in a protein solution (Authelin et al., 2020), the contribution of air bubbles to the protein aggregation caused by dropping stress in the frozen state was not investigated further here.

Although dropping stress induces cavitation and subsequent local high temperatures and high pressures in solutions in vials, cavitation is not likely to happen at −30 °C as the viscosity of the FCM at −30 °C is

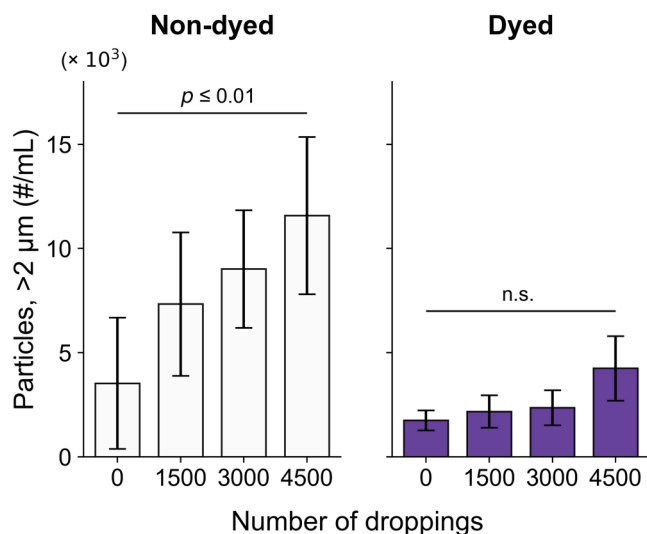


Fig. 7. Concentrations of particles > 2 μm after applying dropping stress to samples frozen in vials coated with dyed CTLA4-Ig. Non-dyed and dyed particles were classified by a SVM-based classifier. n.s.: not significant. Error bars represent the standard deviation of three measurements.

expected to be approximately 2600 Pa·s (Seifert and Friess, 2020). Fang et al. have reported that dropping stress applied to lyophilized drug products caused heat and resulted in increased aggregation (Fang et al., 2021). Thus, a localized high temperature could be induced by dropping stress at -30°C and cause local freeze-thaw conditions. The lack of a significant increase in aggregates at -60°C could be attributed to the cancellation of the heat generated by the dropping stress by the lower temperature. Future work using computational fluid dynamics will provide more insight into heat transfer after the dropping and the reason why the increase in particles due to the dropping stress was observed at -30°C but not at -60°C .

Telikepalli et al. have reported that shipping-like stress damaged a freeze-dried cake of IgG and the number of subvisible particles was increased (Telikepalli et al., 2015). In the present study, the breakup of the frozen solutions rarely occurred and thus was not likely to be a cause of the increased number of aggregates.

The crystallization of excipients is also known to be a factor that can destabilize proteins. P188 can be crystallized in the frozen state. A previous study has demonstrated that the temperature of P188 crystallization (T_{cry}) was approximately -55°C in potassium phosphate buffer, and the preventive effect of P188 on protein aggregation became lower at temperatures below the T_{cry} value (Li et al., 2023). However, in the present study, no increase in protein aggregates was observed at -60°C , which should be lower than the T_{cry} value of P188. This phenomenon can also be explained, as discussed above, because the local freeze-thaw conditions, which are caused by dropping stress-induced heat and are a potential root cause of the aggregation, cannot occur because the generated heat can be compensated for at -60°C .

3.5. Consideration of aggregation caused by dropping stress in the frozen state in real-world situations

The drug substances of therapeutic proteins are often stored in the frozen state. Although drug products are not usually frozen, drug products are sometimes stored in the frozen state in the early stages of development depending on the stability (Authelin et al., 2020). For gene therapy products that have been recently developed, frozen storage is common even for commercial drug products, and the volumes of the drug products are typically one to several milliliters (Peláez et al., 2024). In addition, mRNA-lipid nanoparticle (LNP) vaccines are also stored in the frozen state (Schoenmaker et al., 2021).

The volumes of the bottles or bags used for the storage of drug substances are much larger than the vials used in the present study, which results in slower cooling rates. According to a previous study, the cooling rate of 10 L bottles was $0.5^{\circ}\text{C}/\text{min}$ (Authelin et al., 2020). Our results showed that the number of aggregates $> 5\ \mu\text{m}$ could be increased by dropping stress at -30°C when the samples had been cooled at $-0.1^{\circ}\text{C}/\text{min}$. Although freezing on a larger scale also results in a concentration gradient of the solute (Authelin et al., 2020) and it is difficult to correctly predict the effect of the difference in scale on the stability, there is a distinct possibility that aggregation induced by dropping stress occurs in frozen drug substances.

Previous studies have reported that freeze-thaw stress caused the degradation of viral vectors (Bee et al., 2022; Xu et al., 2022). The aggregation of LNPs caused by freeze-thaw stress has also been observed in a previous study (Ball et al., 2016). Considering that the main cause of aggregation caused by dropping stress in the frozen state was suggested to be local freeze-thaw stress in the present study, the degradation of viral vectors and LNPs in frozen gene therapy products because of dropping stress is possible.

Non-ionic surfactants, including P188, are often added to drug substances and drug products, which would be beneficial to prevent the aggregation caused by dropping stress in the frozen state, as well as to enhance the physical stability in the liquid state. In addition, packaging that can reduce mechanical shock can be used to prevent the aggregation induced by dropping stress. In the present study, the vials were

subjected to dropping up to 4500 times as a stress condition, and the dropping conditions were harsher than the real-world situation. Nevertheless, the results obtained in the present study indicated that aggregation in the frozen state caused by dropping stress may be an issue in the manufacture and transport of frozen therapeutics.

4. Conclusions

In this study, we demonstrated that micron-sized aggregates can be generated by applying dropping stress at -30°C . This aggregation might be related to local freeze-thaw conditions caused by heat induced by the dropping stress. This heat can be compensated for at lower temperatures, and thus an increase in the number of micron-sized aggregates was not observed at -60°C . The cooling rate, which could affect ice crystal size and morphology, was also an important parameter, and a faster cooling rate did not result in a significant increase in the number of aggregates. The addition of P188 was also effective in preventing the aggregation caused by dropping stress in the frozen state. These results indicated that freeze-thaw cycles occurring at ice crystal surfaces generated micron-sized aggregates. Other factors, such as the freeze concentration and the volume of solution, that can affect the stability of the protein in the frozen state will be evaluated in future work. Careful consideration of the destabilization caused by dropping stress in the frozen state will help ensure the safety of biopharmaceuticals.

Funding

The present study was partly supported by JSPS KAKENHI Grant Number 24K18261 to TT and a grant-in-aid from the Japan Agency for Medical Research and Development (AMED) (grants 23ak0101188h0102 to SU and TT and 23ae0121013h0603 to SU).

CRediT authorship contribution statement

Tetsuo Torisu: Writing – review & editing, Writing – original draft, Supervision, Investigation, Data curation, Conceptualization. **Ayuko Maeda:** Investigation, Data curation. **Shuhei Ito:** Investigation, Data curation. **Susumu Uchiyama:** Writing – review & editing, Supervision, Conceptualization.

Declaration of competing interest

The authors declare that they have no known competing financial interests or personal relationships that could have appeared to influence the work reported in this paper.

Acknowledgment

The authors thank Dr. Satoru Yamauchi (ESPEC CORP.) for providing scientific advice. The authors also thank BASF for providing the Poloxamer 188. We would like to thank Monthira Rattanatayaron for her cooperation in the development of the particle classifier. Victoria Muir, PhD, from Edanz (<https://jp.edanz.com/ac>) edited the English text of a draft of this manuscript.

Supplementary materials

Supplementary material associated with this article can be found, in the online version, at [doi:10.1016/j.ejps.2024.106996](https://doi.org/10.1016/j.ejps.2024.106996).

Data availability

Data will be made available on request.

References

- Arsiccio, A., Pisano, R., 2018. Application of the quality by design approach to the freezing step of freeze-drying: building the design space. *J. Pharm. Sci.* 107, 1586–1596. <https://doi.org/10.1016/j.xphs.2018.02.003>.
- Authelin, J.R., Rodrigues, M.A., Tchessalov, S., Singh, S.K., McCoy, T., Wang, S., Shalae, E., 2020. Freezing of biologicals revisited: scale, stability, excipients, and degradation stresses. *J. Pharm. Sci.* 109, 44–61. <https://doi.org/10.1016/j.xphs.2019.10.062>.
- Ball, R.L., Bajaj, P., Whitehead, K.A., 2016. Achieving long-term stability of lipid nanoparticles: examining the effect of pH, temperature, and lyophilization. *Int. J. Nanomed.* 12, 305–315. <https://doi.org/10.2147/IJN.S123062>.
- Bee, J.S., Zhang, Y., Finkner, S., O'Berry, K., Kaushal, A., Phillippi, M.K., DePaz, R.A., Webber, K., Marshall, T., 2022. Mechanistic studies and formulation mitigations of Adeno-associated virus capsid rupture during freezing and thawing: mechanisms of freeze/thaw induced AAV rupture. *J. Pharm. Sci.* 111, 1868–1878. <https://doi.org/10.1016/j.xphs.2022.03.018>.
- Blumel, O., Buecheler, J.W., Hauptmann, A., Hoelzl, G., Bechtold-Peters, K., Friess, W., 2021a. The effect of mAb and excipient cryoconcentration on long-term frozen storage stability - part 2: aggregate formation and oxidation. *Int. J. Pharm. X.* 4, 100109. <https://doi.org/10.1016/j.ijpx.2021.100109>.
- Blumel, O., Anushek, M., Buecheler, J.W., Hoelzl, G., Bechtold-Peters, K., Friess, W., 2021b. The effect of mAb and excipient cryoconcentration on long-term frozen storage stability - part 1: higher molecular weight species and subvisible particle formation. *Int. J. Pharm. X.* 4, 100108. <https://doi.org/10.1016/j.ijpx.2021.100108>.
- Eckhardt, B.M., Oeswein, J.Q., Bewley, T.A., 1991. Effect of freezing on aggregation of human growth hormone. *Pharm. Res.* 8, 1360–1364. <https://doi.org/10.1023/a:101588704365>.
- Fang, W.J., Liu, J.W., Zheng, H.J., Shen, B.B., Wang, X., Kong, Y., Jing, Z.Y., Gao, J.Q., 2021. Protein sub-visible particle and free radical formation of a freeze-dried monoclonal antibody formulation during dropping. *J. Pharm. Sci.* 110, 1625–1634. <https://doi.org/10.1016/j.xphs.2020.10.008>.
- Fang, W.J., Pang, M.J., Liu, J.W., Wang, X., Wang, H., Sun, M.F., 2022. Freeze-dried biopharmaceutical formulations are surprisingly less stable than liquid formulations during dropping. *Pharm. Res.* 39, 795–803. <https://doi.org/10.1007/s11095-022-03235-9>.
- Fast, J.L., Cordes, A.A., Carpenter, J.F., Randolph, T.W., 2009. Physical instability of a therapeutic Fc fusion protein: domain contributions to conformational and colloidal stability. *Biochemistry* 48, 11724–11736. <https://doi.org/10.1021/bi900853v>.
- Hauptmann, A., Hoelzl, G., Loerting, T., 2019. Distribution of protein content and number of aggregates in monoclonal antibody formulation after large-scale freezing. *AAPS PharmSciTech* 20, 72. <https://doi.org/10.1208/s12249-018-1281-z>.
- Jin, M.J., Ge, X.Z., Huang, Q., Liu, J.W., Ingle, R.G., Gao, D., Fang, W.J., 2024. The effects of excipients on freeze-dried monoclonal antibody formulation degradation and sub-visible particle formation during shaking. *Pharm. Res.* 41, 321–334. <https://doi.org/10.1007/s11095-024-03657-7>.
- Kizuki, S., Wang, Z., Torisu, T., Yamauchi, S., Uchiyama, S., 2023. Relationship between aggregation of therapeutic proteins and agitation parameters: acceleration and frequency. *J. Pharm. Sci.* 112, 492–505. <https://doi.org/10.1016/j.xphs.2022.09.022>.
- Lazar, K.L., Patapoff, T.W., Sharma, V.K., 2010. Cold denaturation of monoclonal antibodies. *Mabs* 2, 42–52. <https://doi.org/10.4161/mabs.2.1.10787>.
- Li, J., Sonje, J., Suryanarayanan, R., 2023. Role of poloxamer 188 in preventing ice-surface-induced protein destabilization during freeze-thawing. *Mol. Pharm.* 20, 4587–4596. <https://doi.org/10.1021/acs.molpharmaceut.3c00312>.
- Li, J., Krause, M.E., Tu, R., 2021. Protein Instability at Interfaces During Drug Product Development. Springer, Cham. <https://doi.org/10.1007/978-3-030-57177-1>.
- Liu, L., 2015. Antibody glycosylation and its impact on the pharmacokinetics and pharmacodynamics of monoclonal antibodies and Fc-fusion proteins. *J. Pharm. Sci.* 104, 1866–1884. <https://doi.org/10.1002/jps.24444>.
- Lu, R.M., Hwang, Y.C., Liu, I.J., Lee, C.C., Tsai, H.Z., Li, H.J., Wu, H.C., 2020. Development of therapeutic antibodies for the treatment of diseases. *J. Biomed. Sci.* 27, 1. <https://doi.org/10.1186/s12929-019-0592-z>.
- Oyama, H., Koga, H., Tadokoro, T., Maenaka, K., Shiota, A., Yokoyama, M., Noda, M., Torisu, T., Uchiyama, S., 2020. Relation of colloidal and conformational stabilities to aggregate formation in a monoclonal antibody. *J. Pharm. Sci.* 109, 308–315. <https://doi.org/10.1016/j.xphs.2019.10.038>.
- Peláez, S.S., Mahler, H.C., Vila, P.R., Huwyler, J., Allmendinger, A., 2024. Characterization of freezing processes in drug substance bottles by ice core sampling. *AAPS PharmSciTech.* 25, 102. <https://doi.org/10.1208/s12249-024-02818-6>.
- Pham, N.B., Meng, W.S., 2020. Protein aggregation and immunogenicity of biotherapeutics. *Int. J. Pharm.* 585, 119523. <https://doi.org/10.1016/j.ijpharm.2020.119523>.
- Randolph, T.W., Schiltz, E., Sederstrom, D., Steinmann, D., Mozziconacci, O., Schöneich, C., Freund, E., Ricci, M.S., Carpenter, J.F., Lengersfeld, C.S., 2015. Do not drop: mechanical shock in vials causes cavitation, protein aggregation, and particle formation. *J. Pharm. Sci.* 104, 602–611. <https://doi.org/10.1002/jps.24259>.
- Schoenmaker, L., Witzigmann, D., Kulkarni, J.A., Verbeke, R., Kersten, G., Jiskoot, W., Crommelin, D.J.A., 2021. mRNA-lipid nanoparticle COVID-19 vaccines: structure and stability. *Int. J. Pharm.* 601, 120586. <https://doi.org/10.1016/j.ijpharm.2021.120586>.
- Searles, J.A., Carpenter, J.F., Randolph, T.W., 2001. The ice nucleation temperature determines the primary drying rate of lyophilization for samples frozen on a temperature-controlled shelf. *J. Pharm. Sci.* 90, 860–871. <https://doi.org/10.1002/jps.1039>.
- Seifert, I., Friess, W., 2020. Freeze concentration during freezing: how does the maximally freeze concentrated solution influence protein stability? *Int. J. Pharm.* 589, 119810. <https://doi.org/10.1016/j.ijpharm.2020.119810>.
- Singh, S.K., Kolhe, P., Mehta, A.P., Chico, S.C., Lary, A.L., Huang, M., 2011. Frozen state storage instability of a monoclonal antibody: aggregation as a consequence of trehalose crystallization and protein unfolding. *Pharm. Res.* 28, 873–885. <https://doi.org/10.1007/s11095-010-0343-z>.
- Singh, S.K., Kolhe, P., Wang, W., Nema, S., 2009. Large-scale freezing of biologics—a practitioner's review. Part two: practical advice. *Bioprocess. Int.* 7, 34–42.
- Telikepalli, S., Kumru, O.S., Kim, J.H., Joshi, S.B., O'Berry, K.B., Blake-Haskins, A.W., Perkins, M.D., Middaugh, C.R., Volkin, D.B., 2015. Characterization of the physical stability of a lyophilized IgG1 mAb after accelerated shipping-like stress. *J. Pharm. Sci.* 104, 495–507. <https://doi.org/10.1002/jps.24242>.
- Thorat, A.A., Munjal, B., Geders, T.W., Suryanarayanan, R., 2020. Freezing-induced protein aggregation - role of pH shift and potential mitigation strategies. *J. Control Release* 323, 591–599. <https://doi.org/10.1016/j.jconrel.2020.04.033>.
- Toritsu, T., Maruno, T., Yoneda, S., Hamaji, Y., Honda, S., Ohkubo, T., Uchiyama, S., 2017. Friability testing as a new stress-stability assay for biopharmaceuticals. *J. Pharm. Sci.* 106, 2966–2978. <https://doi.org/10.1016/j.xphs.2017.05.035>.
- Wang, W., Nema, S., Teagarden, D., 2010. Protein aggregation—pathways and influencing factors. *Int. J. Pharm.* 390, 89–99. <https://doi.org/10.1016/j.ijpharm.2010.02.025>.
- Xu, Y., Jiang, B., Samai, P., Tank, S.M., Shameem, M., Liu, D., 2022. Genome DNA leakage of Adeno-Associated virus under freeze-thaw stress. *Int. J. Pharm.* 615, 121464. <https://doi.org/10.1016/j.ijpharm.2022.121464>.
- Yoneda, S., Maruno, T., Mori, A., Hioki, A., Nishiumi, H., Okada, R., Murakami, M., Zekun, W., Fukuhara, A., Itagaki, N., Harauchi, Y., Adachi, S., Okuyama, K., Sawaguchi, T., Torisu, T., Uchiyama, S., 2021. Influence of protein adsorption on aggregation in prefilled syringes. *J. Pharm. Sci.* 110, 3568–3579. <https://doi.org/10.1016/j.xphs.2021.07.007>.